

Uncertainty in water transit time estimation with StorAge Selection functions and tracer data interpolation

Arianna Borriero¹, Rohini Kumar², Tam V. Nguyen¹, Jan H. Fleckenstein^{1,3}, and Stefanie R. Lutz⁴

¹Department of Hydrogeology, Helmholtz-Centre for Environmental Research - UFZ, Leipzig, Germany

²Department of Computational Hydrosystems, Helmholtz-Centre for Environmental Research - UFZ, Leipzig, Germany

³Bayreuth Centre of Ecology and Environmental Research, University of Bayreuth, Bayreuth, Germany

⁴Copernicus Institute of Sustainable Development, Department of Environmental Sciences, Utrecht University, Utrecht, the Netherlands

Correspondence: Arianna Borriero (arianna.borriero@ufz.de)

Abstract. Transit time distributions (TTDs) of streamflow are useful descriptors for understanding flow and solute transport in catchments. Catchment-scale TTDs can be modeled using tracer data (e.g., $\delta^{18}\text{O}$; oxygen isotopes) in inflow and outflows, with StorAge Selection (SAS) functions. However, tracer data are often sparse in space and time, so they need to be interpolated to increase their spatio-temporal resolution. Moreover, SAS functions can be parameterized with different forms, but there is no general agreement on which one should be used. Both of these aspects induce uncertainty in the simulated TTDs, and the individual uncertainty sources as well as their combined effect have not been fully investigated. This study provides a comprehensive analysis of the TTD uncertainty resulting from twelve model setups obtained by combining different interpolation schemes for $\delta^{18}\text{O}$ in precipitation, and distinct SAS functions. For each model setup, we found behavioral solutions with satisfactory model performances for instream $\delta^{18}\text{O}$ (Kling-Gupta Efficiency, $\text{KGE} > 0.57$). Differences in KGE values were statistically significant, thus showing the relevance of the chosen setup for simulating the TTDs. We found a large uncertainty in the simulated TTDs, represented by a large range of variability in the 95% confidence interval of the median transit time varying between 259 and 1009 days across all tested setups. Uncertainty in TTDs was mainly associated with the temporal interpolation of $\delta^{18}\text{O}$ in precipitation, the choice between time-variant and time-invariant SAS functions, flow conditions, and less with the spatial interpolation methods. We discuss the implications of these results for the SAS framework, uncertainty characterization in TTD-based models, and the influence of the uncertainty for water quality and quantity studies.

1 Introduction

Understanding how catchments store and release water of different ages has significant implications for flow and solute transport as water ages encapsulate information about flowpaths characteristics (McGuire and McDonnell, 2006; Botter et al., 2011), contact time of solutes with the soil matrix (Benettin et al., 2015a; Hrachowitz et al., 2016), and vulnerability assessment (Kumar et al., 2020). This plays an important role for water resources protection and management, and requires a tool that can effectively describe catchment-scale transport processes (Rinaldo and Marani, 1987). The age of water in outflows is commonly referred to as transit time (TT), i.e., the time elapsed between the entry of a water parcel into the catchment via precipitation

and its exit via streamflow or evapotranspiration. Accordingly, the transit time distribution (TTD) describes the whole spectrum of the transit times in outflows (Botter et al., 2005; Van der Velde et al., 2010). Early studies have often assumed simplified steady-state transport models, resulting in time-invariant TTDs (Niemi, 1977; Rinaldo et al., 2006). However, experimental simulations showed that TTDs are time-variant due to the variability in meteorological forcing (Botter et al., 2010; Hrachowitz et al., 2010; Heidbüchel et al., 2020) and activation/deactivation of flowpaths in response to varying hydrologic conditions (Ambroise, 2004; Heidbüchel et al., 2013). Recent research has introduced new models for representing time-variant TTDs, for example allowing for the estimation of TTDs without making prior assumptions about their shape (Kirchner, 2019; Kim and Troch, 2022), or via parameterization of the StorAge Selections (SAS) functions (Rinaldo et al., 2015; Harman, 2019). SAS functions describe how catchments selectively remove water of different ages from storage for outflows, and have led to a new framework of non-stationary transport models based on water age, which have been successfully applied in various transport modelling studies (Benettin et al., 2015b; Queloiz et al., 2015; Kim et al., 2016; Lutz et al., 2017; Wilusz et al., 2017; Nguyen et al., 2021).

Model-based TTDs are subjected to uncertainty, which limits their ability for decision support. In general, model prediction uncertainty stems from model inputs, structure, and parameters (Beven and Freer, 2001). As TTDs are not directly observable, conservative environmental tracers (e.g., $\delta^{18}\text{O}$; oxygen isotopes) in inflow and outflows are commonly used to infer water ages (Hrachowitz et al., 2013; Birkel and Soulsby, 2015; Stockinger et al., 2015). Long-term, high-frequency tracer data with appropriate spatial distribution are generally recommended for sufficient understanding of TTD dynamics across a wide range of fast and heterogeneous hydrological behaviors (Kirchner et al., 2004; Danesh-Yazdi et al., 2016; von Freyberg et al., 2017). Therefore, the lack of appropriate tracer data coverage can hamper our understanding of TTD dynamics at the desired resolution (McGuire and McDonnel, 2006). Additionally, uncertainty in the driving hydroclimatic fluxes such as precipitation, discharge, and evapotranspiration could propagate into the uncertainty of the modelling results. Further uncertainty emerges from the model structure due to the difficulty in representing physical processes because of our incomplete knowledge of complex reality (Ajami et al., 2007). Finally, specification of model parameters is also an important source of uncertainty (Beven, 2006; Kirchner, 2006), as the best-fit parameters may suffer from equifinality (Schoups et al., 2008).

A few studies have investigated the uncertainty in the estimated TTDs with SAS models. Danesh-Yazdi et al. (2018) and Jing et al. (2019) have analysed the effect of interactions between distinct flow domains, external forcing and recharge rate on resulting TTDs. Several works (Benettin et al., 2017; Wilusz et al., 2017; Rodriguez et al., 2018, 2021) have explored model parameter uncertainty, and suggested that additional types of tracers, data on physical characteristics of the catchment, and parsimonious parameterization may help to further reduce parametric uncertainty in the SAS modelling approach. More recently, Buzacott et al. (2020) investigated how gap-filling of the $\delta^{18}\text{O}$ record in precipitation propagated uncertainty into the simulated mean water transit time (MTT), i.e., the average time it takes for water to leave the catchment (McDonnel et al., 2010).

Despite the studies cited above, there are other aspects particularly significant for SAS modelling causing uncertainty in the simulated TTDs, which have not yet been thoroughly investigated. First, isotope data are generally sparse globally in space and time (von Freyberg et al., 2022), due to laborious and costly sampling campaigns limited to well-equipped areas (Tetzlaff

et al., 2018). As SAS models require continuous time series of input tracer data, different methods for temporal interpolation could be used to fill gaps in isotope values in precipitation; consequently, the interpolated input data are subject to uncertainty. Furthermore, the input data of SAS models are influenced by whether the tracer data in precipitation are collected at a single location within the catchment, or at multiple locations. In the latter scenario, there is a need to account for the spatial variability of tracer composition in precipitation, which is commonly done via spatial interpolation. Choosing data from one approach (i.e., tracer data from a single location) over the other (i.e., multiple tracer data spatially interpolated) can potentially result in different resulting TTDs. Finally, SAS functions, employed to model TTDs, must be parameterized and their functional forms need to be specified a-priori. Commonly used forms are the power law (Benettin et al., 2017; Asadollahi et al., 2020), beta (van der Velde et al., 2012; Drever and Hrachowitz, 2017) and gamma (Harman, 2015; Wilusz et al., 2017) distributions. However, there is no general agreement on which SAS function should be used since the hydrological processes that control the patterns and dynamics of the subsurface vary across catchments. Therefore, the most convenient approach is to simply rely on a specific parameterization over another, and estimate its parameters (Harman, 2015). All of these aspects, related to model input, structure and parameter, induce uncertainty in the simulated TTDs. To date, the role of these individual uncertainty sources and their combined effect on the modeled TTDs have not been adequately discussed.

This study bridges the aforementioned gaps by specifically exploring the combined effect of sparse input tracer data and model parameterizations on the simulated TTDs. We investigated TTD uncertainty using a SAS-based catchment-scale transport model applied to the Upper Selke catchment, Germany. We evaluated TTDs resulting from twelve model setups obtained by combining distinct interpolation techniques of $\delta^{18}\text{O}$ in precipitation, and parameterizations of SAS functions. For each model setup, we searched for behavioral parameter sets (i.e., those providing acceptable predictions) based on model performance for instream $\delta^{18}\text{O}$, and evaluated the sources of uncertainty, as well as their combined effects, in the modeled TTDs. Overall, our results provide new insights into the uncertainty characterization of TTDs, particularly in the absence of high-frequency tracer data, and the use of SAS functions, as well as implications of TTDs uncertainty on water quantity and quality studies.

2 Study area and data

The Upper Selke catchment is located in the Harz Mountains in Saxony-Anhalt, central Germany (Fig. 1). The study site is part of the Bode region, an intensively monitored area within the TERENO (TERrestrial ENvironmental Observatories; Wollschläger et al., 2017) network. The catchment has a drainage area of 184 km², the altitude ranges between 184 and 594 m above mean sea level, and the mean slope is 7.65%. Land use is dominated by forest (broadleaf, coniferous and mixed forest) and agricultural land (winter cereals, rapeseed and maize), representing 72% and 21% of the catchment, respectively. The soil is largely composed of cambisols and the underlying geology consists of schist and claystone, resulting in a predominance of relatively shallow flowpaths (Dupas et al., 2017; Yang, J. et al., 2018).

Daily hydroclimatic and monthly tracer data in the Upper Selke were available for the period between February 2013 and May 2015. Precipitation (P) was taken from the German weather service, while discharge (Q) and evapotranspiration (ET) were

simulated data obtained from the mesoscale Hydrological Model (mHM; (Samaniego et al., 2010; Kumar et al., 2013)) since continuous measurements were not available for the given outlet and period. A thorough evaluation of mHM performance for past measurements have been conducted in previous studies (Zink et al., 2017; Yang, X. et al., 2018; Nguyen et al., 2021). The average annual P, Q and ET are 703, 108, 596 mm, respectively. The area is characterized by high flow during November-May (average Q = 0.88 m³/s) and low flow during June-October (average Q = 0.42 m³/s). Evapotranspiration is higher in June (109 mm/month) and lower in December (10 mm/month). The average monthly temperature ranges from -0.7°C in January to 17°C in July. The $\delta^{18}\text{O}$ values in precipitation ($\delta^{18}\text{O}_P$) and in streamflow ($\delta^{18}\text{O}_Q$) at monthly resolution were taken from Lutz et al. (2018) (Fig. S1). Values of $\delta^{18}\text{O}_P$ were used in the form of "raw" (i.e., values collected at the catchment outlet) and processed (i.e., values collected at multiple location and spatially interpolated using kriging) data (see Section 3.2 for more details). The variability in $\delta^{18}\text{O}_P$ was larger than $\delta^{18}\text{O}_Q$ (Fig. S1) because of the damping of the precipitation signal due to mixing and dispersion within the catchment. Temperature dependence caused more depleted (i.e., more negative) $\delta^{18}\text{O}_P$ in winter than in summer (Fig. S1).

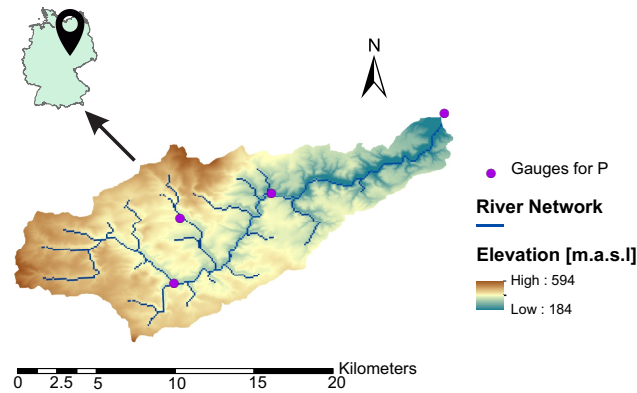


Figure 1. Upper Selke catchment with precipitation sampling points (purple dots), river network (blue lines), and elevation in meters above sea level as colored map; location of the Upper Selke catchment in Germany (upper left corner).

3 Methods

3.1 Catchment-scale transport model

In this study, we used the *tran-SAS* model (Benettin and Bertuzzo, 2018) for describing the catchment-scale water mixing and solute transport based on SAS functions. The catchment was conceptualized as a single storage $S(t)$ (mm), whose water-age balance can be expressed as follows (Benettin and Bertuzzo, 2018):

$$S(t) = S_0 + V(t) \quad (1)$$

$$110 \quad \frac{\partial S_T(T, t)}{\partial t} + \frac{\partial S_T(T, t)}{\partial T} = P(t) - Q(t) \cdot \Omega_Q(S_T, t) - ET(t) \cdot \Omega_{ET}(S_T, t) \quad (2)$$

$$\text{Initial condition: } S_T(T, t = 0) = S_{T_0}(T) \quad (3)$$

$$\text{Boundary condition: } S_T(0, t) = 0 \quad (4)$$

where S_0 (mm) is the initial storage, $V(t)$ (mm) are the storage variations, $P(t)$ (mm/d), $Q(t)$ (mm/d), and $ET(t)$ (mm/d) are precipitation, discharge and evapotranspiration, respectively, $S_T(T, t)$ (mm) is the age-ranked storage, $S_{T_0}(T)$ (mm) is the initial age-ranked storage, and $\Omega_Q(S_T, t)$ (-) and $\Omega_{ET}(S_T, t)$ (-) are the cumulative SAS functions for Q and ET , respectively.

By definition, the TTD of streamflow $p_Q(T, t)$ (d^{-1}) is calculated as follows (Benettin and Bertuzzo, 2018):

$$p_Q(T, t) = \frac{\partial \Omega_Q(S_T, t)}{\partial S_T} \cdot \frac{\partial S_T}{\partial T}. \quad (5)$$

The isotopic signature in streamflow $C_Q(t)$ (‰) can be obtained from (Benettin and Bertuzzo, 2018):

$$C_Q(t) = \int_0^{+\infty} C_S(T, t) \cdot p_Q(T, t) \cdot dT \quad (6)$$

120 where $C_S(T, t)$ (‰) is the isotopic signature of a water parcel in storage. Equations 5 and 6 also apply for ET .

In this study, we tested three SAS parameterizations: the power law time-invariant (PLTI; Eq. 7 (Queloz et al., 2015)), power law time-variant (PLTV; Eq. 8 (Benettin et al., 2017)), and time-invariant beta (BETATI; Eq. 9 (Drever and Hrachowitz, 2017)) distribution. Here, they are expressed as probability density functions in terms of the normalized age-ranked storage $P_S(T, t)$ (-), also known as fractional SAS functions (fSAS):

$$125 \quad \omega(P_S(T, t), t) = k \cdot (P_S(T, t))^{k-1} \quad (7)$$

$$\omega(P_S(T, t), t) = k(t) \cdot (P_S(T, t))^{k(t)-1} \quad (8)$$

$$\omega(P_S(T, t), t) = \frac{(P_S(T, t))^{\alpha-1} \cdot (1 - P_S(T, t))^{\beta-1}}{B(\alpha, \beta)}. \quad (9)$$

The parameters k , α and β determine the catchment's water age preference for outflows, while $B(\alpha, \beta)$ is the two-parameter beta function. If $k < 1$, or if $\alpha < 1$ and $\beta > 1$, the system tends to discharge young water. If $k > 1$, or if $\alpha > 1$ and $\beta < 1$, the catchment preferably releases old water. The case of $k = 1$ or $\alpha = \beta = 1$ describes no selection preference (i.e., complete water mixing). PLTV is characterized by $k(t)$ varying linearly over time between two extremes k_1 and k_2 as a function of the catchment wetness w_i (-), i.e., $w_i(t) = (S(t) - S_{min}) / (S_{max} - S_{min})$, where S_{min} and S_{max} are the minimum and maximum storage values over the entire period.

3.2 Interpolation techniques for $\delta^{18}\text{O}$ in precipitation

We tested the model with two spatial and two temporal interpolation methods of tracer data to explore the TTD uncertainty resulting from model input. To evaluate the effect of the spatial interpolation, we first set a base case using monthly raw $\delta^{18}\text{O}_p$

taken from Lutz et al. (2018), corresponding to the values collected at a single location, i.e. the catchment outlet at Meisdorf station. Second, we used the spatially interpolated $\delta^{18}\text{O}_P$ estimates from Lutz et al. (2018), which are based on raw observations from 24 precipitation collectors spread over the larger area of the Bode region. The spatial interpolation in Lutz et al. (2018) was conducted using kriging with altitude as an external drift. The kriged $\delta^{18}\text{O}_P$ were further weighted with spatially distributed monthly precipitation to obtain representative estimates for the study region.

SAS model results are sensitive to the choice of the temporal resolution of input tracer data, and shorter time steps are generally recommended to achieve a satisfactory level of detail (Benettin and Bertuzzo, 2018). Additionally, a forward Euler scheme was employed to solve Eq. 2, whose precision increases with high frequency time steps. For these reasons, we reconstructed daily $\delta^{18}\text{O}_P$ estimates from monthly values with two different interpolation schemes. First, we used a step function in which the values between two consecutive samples assumed the value of the last sample. Second, we used a sine interpolation based on the assumption that $\delta^{18}\text{O}_P$ values follow a seasonal cycle (Fig. S1 in the Supplement, (Feng et al., 2009)), whose signature over a period of one year can be described by (Kirchner, 2016):

$$\delta^{18}\text{O}_P(t) = a_P \cdot \cos(2 \cdot \pi \cdot f \cdot t) + b_P \cdot \sin(2 \cdot \pi \cdot f \cdot t) + k_P \quad (10)$$

where a and b are regression coefficients (-), t is the time (decimal years), f is the frequency (yr^{-1}) and k is the vertical offset of the isotope signal (‰). The coefficients a and b were estimated by fitting Eq. 10 to monthly $\delta^{18}\text{O}_P$ values using the iteratively re-weighted least squares (IRLS) estimation (von Freyberg et al., 2018). Subsequently, the estimated regression coefficients were used in Eq. 10 to obtain isotope data at daily frequency. Figure S2 in the Supplement displays the simulated kriged and raw $\delta^{18}\text{O}_P$ values via step function and sine interpolation.

3.3 Experimental design

In this study, different scenarios were used to quantify uncertainty in the modeled results. We tested twelve setups composed of three SAS functions (PLTI, PLTV, BETATI), two temporal (step and sine function) and two spatial (raw and kriging values) interpolation techniques (Table 1). For each setup, we performed a Monte-Carlo experiment by running the model with 10,000 parameter sets generated by the Latin Hypercube Sampling (LHS, McKay et al., 1979). Model parameters and their search ranges are shown in Table 2.

A 5 years warm-up period (i.e., repetition of the input data) from February 2008 to January 2013 was performed to reduce the impact of the model initialization. The period from February 2013 to May 2015 was used to infer behavioral model parameters (i.e., parameter sets giving acceptable predictions), and subsequently to interpret the model results. The initial concentration of $\delta^{18}\text{O}$ in storage was set to 9.2 ‰ coinciding with the mean $\delta^{18}\text{O}_Q$ over the study period.

The informal likelihood of the Sequential Uncertainty Fitting Procedure (SUFI-2, Abbaspour et al., 2004) was applied to account for uncertainty in the SAS parameter sets and resulting modeled estimates. In SUFI-2, the uncertainty in model parameters and simulated results is represented by a uniform distribution, which is gradually reduced until a specific criterion is reached. In our study, we calibrated the values of model parameters until the predicted output matched the measured tracer data to a satisfactory level, defined by an objective function. We employed as objective function the Kling-Gupta efficiency

Table 1. List of model setups.

setup	interpolation	SAS function
a	step function kriged $\delta^{18}\text{O}_P$	PLTI
b		PLTV
c		BETATI
d	step function raw $\delta^{18}\text{O}_P$	PLTI
e		PLTV
f		BETATI
g	sine function kriged $\delta^{18}\text{O}_P$	PLTI
h		PLTV
i		BETATI
j	sine function raw $\delta^{18}\text{O}_P$	PLTI
k		PLTV
l		BETATI

Table 2. Model parameters and search ranges.

SAS parameter	Symbol	Unit	Lower Bound	Upper Bound
Discharge SAS parameter	k_Q	[-]	0.1	2
	k_{Q1}	[-]	0.1	2
	k_{Q2}	[-]	0.1	2
	α	[-]	0.1	2
	β	[-]	0.1	2
Evapotranspiration SAS parameter	k_{ET}	[-]	0.1	2
Initial storage	S_0	[mm]	300	3000

(KGE, Gupta et al., 2009), and once the criterion of $\text{KGE} \geq 0.5$ was satisfied, we defined a set of behavioral solutions for each
170 model setup. However, since the aim of this study is to investigate the impact of various sources of uncertainty on simulated
outputs, rather than to determine the best model setup based on the model efficiency, we decided to set a fixed sample size
and narrow down those solutions generated by SUFI-2 in the previous step. Setting a fixed sample size ensures comparability
of results across the twelve tested setups, as different sample sizes could influence the uncertainty analysis. For example, the
greater the number of behavioral solutions, the wider the uncertainty band. At the same time, by fixing the sample size, we can
175 still meet the requirement of a minimum acceptable KGE value (i.e., $\text{KGE} \geq 0.5$).

In this study, we determined the final behavioral solutions by using a fixed sample size that corresponds to the best 5%
parameter sets and modeled results in terms of KGE. Finally, we constructed the 95% confidence intervals (CI) based on the
2.5% and 97.5% CIs of the cumulative distribution in the time series of parameters and output variables (Abbaspour et al.,
2004) to refine the limits of the behavioral solutions. In our experimental setup, the main output variables were the instream
180 $\delta^{18}\text{O}$ signature and backward median transit time (TT_{50} (days), i.e., the maximum time elapsed until the youngest 50% of the
infiltrated water is transferred to the outflow). Time series of TT_{50} were extracted directly from daily TTDs (Eq. 5) and used
as a metric for the streamflow age. This was done because TTDs are typically skewed with long tails (Kirchner et al., 2001),

hence the median is often a more suitable metric than, for example, MTT as it is less impacted by the poor identifiability of the older water components (Benettin et al., 2017).

185 4 Results

4.1 Simulated $\delta^{18}\text{O}$ in streamflow and model performances

Modeled $\delta^{18}\text{O}$ in streamflow ($\delta^{18}\text{O}_Q$) represented by the 95% confidence interval (CI) in the ensemble solution are displayed in Fig. 2. The results reveal how the predicted $\delta^{18}\text{O}_Q$ values enveloped the measured isotopic signature by reproducing its seasonal fluctuations, with depleted (i.e., more negative) values in winter and enriched (i.e., less negative) values in summer.

190 However, the second half of the study period was characterized by more enriched predicted $\delta^{18}\text{O}_Q$ values than the measured ones. Although the behavioral parameter sets were able to capture the seasonal isotopic trend, they poorly reproduced the exact values; therefore, the ensemble simulations are characterized by a non-negligible uncertainty.

Figure 2 shows the distinct effects of the interpolated input tracer data and model parameterization on the simulated $\delta^{18}\text{O}_Q$ values. The step function interpolation generated an erratic isotopic signature in streamflow with flashy fluctuations, explicitly visible in Fig. 2c and f. On the other hand, the sine interpolation of $\delta^{18}\text{O}_P$ values yielded a smooth response in the simulated $\delta^{18}\text{O}_Q$ values (Fig. 2g-l). The sine interpolation also induced larger seasonal tracer cycle amplitudes (Fig. 2g-l) than those produced when using the step function (Fig. 2a-f). Conversely, no clear visual difference was found between kriged (Fig. 2a-c and g-i) and raw (Fig. 2d-f and j-l) $\delta^{18}\text{O}_P$ samples as their general patterns match (Fig. S2 in the Supplement). Likewise, distinct SAS parameterizations did not produce remarkable differences in the simulated $\delta^{18}\text{O}_Q$ values, although PLTV generally yielded 200 simulations that better enveloped the measured isotopic signature (Figs. 2b, e, h and k).

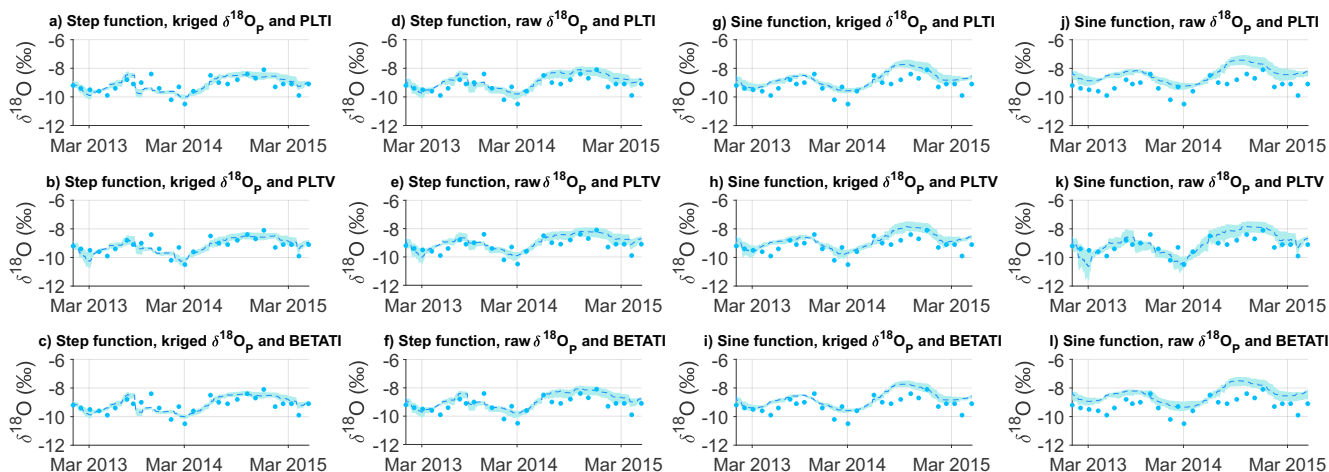


Figure 2. Predicted $\delta^{18}\text{O}$ values in streamflow. Dark blue filled circles represent the observed data; the light blue line and the shaded area represent, respectively, the ensemble mean of all possible solutions and their range according to the 95% CI.

Despite the differences in the predicted $\delta^{18}\text{O}_Q$ values, all simulations can be considered satisfactory given the KGE values ranging between 0.57 and 0.75, across all tested setups (Fig. 3). These performances can be classified from intermediate (Thiemig et al., 2013) to good (Andersson et al., 2017; Sutanudjaja et al., 2018). When considering the best fit, the combination of the step function interpolation and raw $\delta^{18}\text{O}_P$ values performed best. Additionally, PLTV generally yielded slightly better KGE values than PLTI and BETATI when grouping the setups with the same interpolation technique of $\delta^{18}\text{O}_P$. Differences in the mean KGEs were statistically insignificant (t-test with p-values > 0.05) between setups h and i (Table 1), and this largely agrees with the visual analysis (Fig. 3). Contrarily, the differences in the mean KGE values of the remaining setups were statistically significant (p-values < 0.05), indicating that a priori methodological choice (i.e., interpolation techniques of $\delta^{18}\text{O}_P$ values and/or SAS parameterization) strongly impact on the overall results. Nonetheless, this does not mean that we can clearly identify the most suitable setup, but there is need to carefully analyze the multiple potential choices in SAS parameterization and tracer data interpolations, and to evaluate the uncertainty range in modeled predictions.

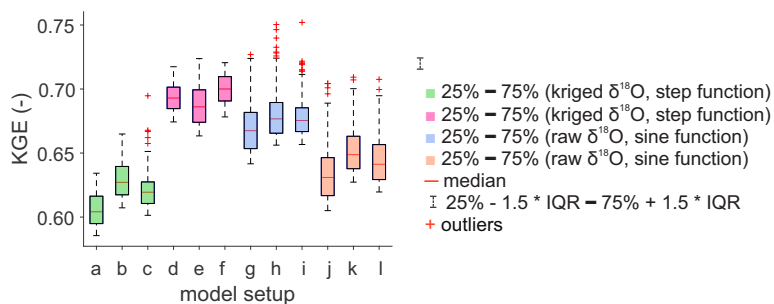


Figure 3. Boxplot of model performance ranges in behavioral solutions. The letters on the x-axis refer to the model setup type according to Table 1. Boxplots filled with the same colors represent model setups characterized by the same interpolation scheme in space and time. On each box, the central red line indicates the median, and the bottom and top edges of the box indicate the 25th and 75th percentiles respectively, namely the interquartile range (IQR). The whiskers extend to the most extreme data points not considered outliers which are 25th percentile minus 1.5 times IQR and 25th percentile plus 1.5 times IQR, respectively. The outliers are plotted individually using the red '+' mark.

Ranges of the behavioral SAS parameters for the tested setups are summarized in Table S1 in the Supplement. Parameters for the SAS functions of Q (i.e., k_Q , k_{Q1} , k_{Q2} , α and β) were different across the setups although, in general, they were relatively narrow and well identified. However, the behavioral parameters were better constrained when using the step function interpolation since their 95% CI was, on average, 26% narrower than that provided by the sine interpolation, across all the SAS parameterizations. The parameters k_{Q1} and α were also better identified than k_{Q2} and β , since their 95% CI was, on average, 67% narrower, across all tested setups. Conversely, there was no clear difference in the parameters ranges when using kriged or raw $\delta^{18}\text{O}_P$ values. The evapotranspiration parameter (i.e., k_{ET}) was poorly identified in all setups as any value in the search range provided equally good results. The initial storage (i.e., S_0) was only partially constrained as any value between 340 mm and 2895 mm was considered acceptable.

4.2 Simulated transit times and model uncertainty

Figure 4 illustrates the 95% CI of the behavioral solutions for the predicted median transit time (TT_{50}). The results show that the model simulated largely different ranges of TT_{50} based on the tested setups. When using PLTI and BETATI, the 95% CI was relatively stable with small fluctuations throughout the simulation period, compared to PLTV (Fig. 4a, c, d, f, g, i, j and 225 1). However, minor differences emerged across the simulated TT_{50} as a result of the distinct interpolation techniques used for $\delta^{18}O_P$. The 95% CI of TT_{50} was on average larger by 36%, across all tested setups, when using raw $\delta^{18}O_P$ (Fig. 4d-f and j-l) rather than kriged $\delta^{18}O_P$ (Fig. 4a-c and g-i). This was especially visible when the step function was used (Fig. 4a-f). Moreover, the sine function generated a 95% CI of TT_{50} being on average 62% narrower across all tested setups (Fig. 4g-l) with respect to the step function (Fig. 4a-f). These differences were more evident for high flow conditions. In addition, the behavioral solutions 230 obtained with the sine function (Fig. 4g-l) were more skewed towards shorter mean TT_{50} values, across all tested setups, than those of the step function (Fig. 4a-f).

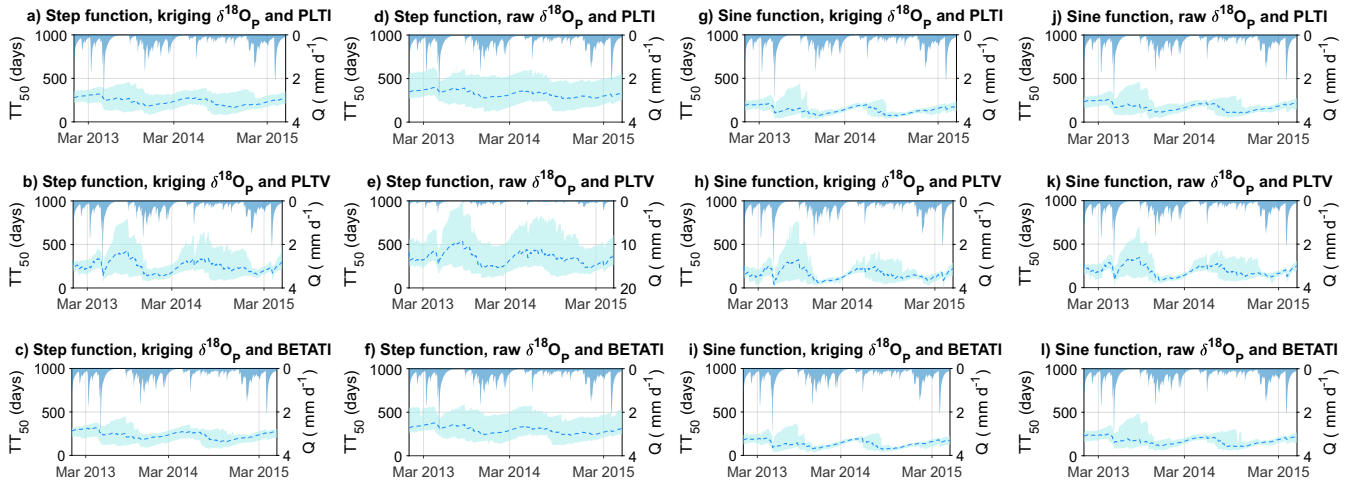


Figure 4. Predicted TT_{50} of streamflow; the light blue line and the shaded area represent, respectively, the ensemble mean of all possible solutions and their range according to the 95% CI.

Behavioral solutions obtained with PLTV revealed a similar pattern regardless of the interpolation employed (Fig. 4b, e, h and k). Nonetheless, there was a noticeable difference in the 95% CI of TT_{50} under distinct flow regimes. During low flows and dry periods (i.e., summer and autumn), the time series of predicted TT_{50} showed large uncertainties ranging at most between 235 259 and 1009 days across the different setups (Fig. 4e). Conversely, during high flows (i.e., winter and spring), the 95% CI was much narrower and varied at least between 129 and 160 days (Fig. 4h). The large 95% CI and the notable differences across the tested setups highlight the sensitivity and, in turn, the uncertainty of predicted TT_{50} to the model parameterization, temporal interpolation of input data and hydrologic conditions. In contrast, the use of raw or kriged $\delta^{18}O_P$ samples produced smaller differences as the trend in the estimated TT_{50} was very similar. Thus, the spatial interpolation technique impact less the water 240 age simulations. However, the 95% CI of TT_{50} was larger when using raw rather than kriged $\delta^{18}O_P$ values.

In general, the variability of the predicted TT_{50} was controlled by the hydrological state of the system (Fig. 4). High discharge events reduced the TT_{50} values, while low flow periods were associated with a longer estimated TT_{50} . This is expected as streamflow during high (low) flows is dominated by near-surface runoff (groundwater) with shallow (deep) flowpaths leading to a shorter (longer) TT_{50} . Such differences were particularly visible with PLTV (Fig. 4b, e, h, and k) as the exponent $k_Q(t)$ shift the water selection preference over time as a function of the wet/dry conditions. This resulted in the variability of TT_{50} being more pronounced than that of PLTI and BETATI, whose SAS parameters for Q are constant over time.

4.3 Catchment-scale water release

SAS functions provided valuable insights into the catchment-scale water release dynamics. Figure 5 presents the behavioral solutions releasing water of different ages, and shows that the catchment generally experienced a stronger affinity for realising young water (i.e., $k_Q < 1$, or $\alpha < 1$ and $\beta > 1$), rather than old water (i.e., $k_Q > 1$, or $\alpha > 1$ and $\beta < 1$). These findings are in agreement with other studies in the Upper Selke (Winter et al., 2020; Nguyen et al., 2021). Nonetheless, there were differences in the water release scheme when comparing various combinations of SAS functions and spatio-temporal interpolation techniques of isotopes. The use of PLTV resulted in a substantial number of solutions, approximately 50% of all behavioral solutions, suggesting a preference for both young and old water. On the other hand, only a few solutions showed affinity for old water release, and this was more prominent when using the sine interpolation technique, raw $\delta^{18}O_P$ values and PLTI across all tested setups.

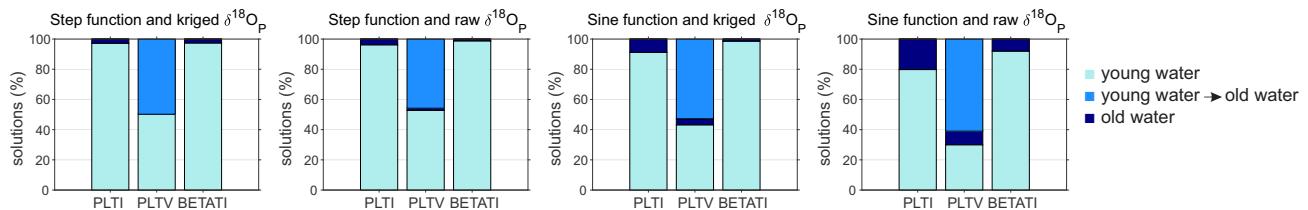


Figure 5. Percentage of behavioral solutions releasing water of different ages.

5 Discussion

5.1 Uncertainty in TTD modelling

In this study, we characterized the TTD uncertainty arising from some significant and critical aspects for the SAS modelling. These aspects are also the most directly linked to data interpolation and SAS parameterization that we explored in this work. The uncertainty analysis has been carried out across the twelve tested setups corresponding to different combinations of spatio-temporal data interpolation techniques and SAS parameterizations. Our results show that the uncertainty (i.e., 95% CI) of the

simulated TT_{50} (Fig. 4) was firmly dependent on the choice of model setup, and we found that the 95% CI is primarily sensitive to the SAS parameterizations as well as temporal interpolation of $\delta^{18}O_p$, and less on the spatial interpolation of $\delta^{18}O_p$.

265 Uncertainty in the simulated TT_{50} differed considerably between time-invariant (i.e. PLTI and BETATI; Fig. 4a, c, d, f, g, i, j and l) and time-variant (i.e., PLTV; Fig. 4b, e, h and k) SAS functions, thus a large sensitivity is associated with the choice of the SAS parameterization. For example, PLTI and BETATI explicitly assume constant water selection preference over time as these functions do not consider temporal variability of the catchment wetness. As a consequence, the resulting simulations had a moderately stable 95% CI in TT_{50} with smaller fluctuations compared to those of PLTV. Hence, the model setup with PLTI
270 and BETATI could be appropriate in catchments experiencing a less pronounced seasonality in streamflow and precipitation.

On the other hand, including an explicit time dependence in the SAS function strongly affected the 95% CI of TT_{50} . PLTV produced a wider 95% CI notably during low flow conditions, which can hinder the ability of the TTDs to provide robust insights on flow and solute transport behaviors in the study area during low flow conditions. This highlights the need to further constrain PLTV with additional data, which could involve obtaining tracer data at a finer resolution or additional information
275 on the evapotranspiration and initial storage. In addition, the exceptionally old flow components associated with a very large 95% CI of TT_{50} might be a distortion of the actual TT_{50} values, which can usually be more reliably estimated using radioactive tracers rather than stable isotopes (Visser et al., 2019). Hence, PLTV-based TT_{50} greater than the observed period (828 days) should be interpreted carefully. However, in this study we discussed the fractional (fSAS) functions, while another form of the SAS functions, such as the rank SAS (rSAS) functions, may have different uncertainty characteristics. This is mainly due to
280 the difference in how the storage is considered, because fSAS functions are expressed as function of the normalized age-ranked storage, which is equal to the cumulative residence time, while rSAS functions depend on the age-ranked storage, which is the volume of water in storage ranked from youngest to oldest (Harman, 2015).

Likewise, the high-frequency reconstruction of $\delta^{18}O_p$ estimates from monthly values via interpolation created further uncertainty that would not arise when using real high-frequency data. The sine interpolation poorly reproduced flashy rainfall events
285 and only captured the average damped trend of the observed $\delta^{18}O_p$ samples (Fig. S2 in the Supplement). Hence, related results must be interpreted with caution as tracer data uncertainty may conceal a more pronounced hydrological response (Dunn et al., 2008; Birkel et al., 2010; Hrachowitz et al., 2011). Contrarily, the step function interpolation preserved the maxima in the monthly observed $\delta^{18}O_p$ values, and reproduced their variation correctly. Nonetheless, the results obtained in this study are based on this particular isotope dataset, while the sine interpolation may be better applicable in other circumstances. Overall,
290 the temporal interpolation of tracers resulted in largely differing reconstructed input data depending on whether the step function or sine interpolation were used (Fig. S2 in the Supplement). This explains why the simulated TT_{50} is different between the two interpolations or, in other words, why the uncertainty in TT_{50} is large.

On the contrary, the spatial interpolation method did not strongly affect the simulated TT_{50} as the trend in the time series was similar when using kriged (Fig. 4a-c and g-i) or raw (Fig. 4d-f and j-l) $\delta^{18}O_p$. This could be attributed to minor differences
295 between kriged and raw isotopes (Figs. S1 and S2 in the Supplement). Nonetheless, there was a larger 95% CI of TT_{50} when using raw rather than kriged $\delta^{18}O_p$, and this was particularly visible when the step function interpolation was used (Fig. 4a-

f). Therefore, the spatial interpolation of $\delta^{18}\text{O}$ in precipitation from different locations resulted in an apparent reduction of uncertainty in TT_{50} .

In addition, we found that the uncertainty was larger under dry conditions when lower flow and longer TT_{50} were observed. This was especially visible when using the time-variant SAS function (Fig. 4b, e, h and k). It might be due to the fact that under wet conditions, there is a high level of hydrologic connectivity within the catchment (Ambroise, 2004; Blume and van Meerveld, 2015; Hrachowitz et al., 2016), which results in nearly all flow paths being active and contributing to the streamflow that, ultimately, may make TT_{50} values easier to constrain. Conversely, under dry conditions, when there is low connectivity within the catchment, only certain flow paths are active, i.e., usually those carrying older water to the stream (Soulsby and Tetzlaff, 2008; Jasechko et al., 2017). Hence, these flows are less uniform, making it more challenging to constrain their older water ages. Similarly, Benettin et al. (2017) found higher uncertainty in the simulated SAS-based median water ages during drier periods, potentially due to higher uncertainty in the total storage. Moreover, non-SAS functions studies have observed major uncertainties and deviations from observations in lumped modeled results during low flow conditions (Kumar et al., 2010). This was primarily due to the lack of spatial variability of catchment characteristics in lumped models, a critical factor controlling low flow regimes in rivers.

The dissimilarities in the simulated TT_{50} across the tested setups underline the importance of accounting for uncertainty in model-based TTDs. The uncertainty analysis with SUFI-2 performed in this study was essential to best describe the parameter identifiability and bounds of the behavioral solutions of each output variable. Furthermore, our results highlight the importance of gaining tracer datasets of good quality, meaning tracer data with a finer resolution, and, possibly, employing the "true" model parameterization which correctly describes the catchment-specific storage and release dynamics. The second point can be defined according to a precise conceptual knowledge of the catchment's functioning and information from previous studies in similar catchments.

5.2 TTD modelling: advantages and limitations

Our results provide visually plausible seasonal fluctuations of the predicted $\delta^{18}\text{O}_Q$ samples (Fig. 2), and satisfactory KGE values (Fig. 3), despite the uncertainty arising from model inputs, structure and parameters. The good match with observations provides high confidence in the simulated TT_{50} for the Upper Selke. The magnitude of the uncertainty resulting from different setups cannot be generalized, but the overall approach for uncertainty assessment presented here could be extended to other areas and TTD studies. However, we recognize some limitations and indicate below possible reasons and, in turn, improvements that future work could achieve.

First, the limited length of the $\delta^{18}\text{O}$ time series might not describe the system accurately, hence implementing longer time series could improve the parameter identifiability and provide a more accurate estimation of the TTDs. Second, this study relied on stable water isotopes, which might underestimate the tails of the TTDs (Stewart et al., 2010; Seeger and Weiler, 2014; Wang et al., 2022). Possible advancements could be reached by using decaying tracers varying over a larger timescale than stable water isotopes (e.g., tritium, (Stewart et al., 2012; Morgenstern et al., 2015)), and imparting more information on old water. Next, future work should retrieve more information on ET and the initial storage S_0 , whose parameters were poorly identified.

However, this issue is common in transport studies that rely on measurements of instream stable water isotopes (Benettin et al., 2017; Buzacott et al., 2020). As a way forward, information on the *ET* isotopic compositions might help better constrain *ET* parameters and assess their affinity for young/old water. Regarding constraining the range of S_0 , further information can be gained from geophysical surveys in the study areas or groundwater modeling, as well as using decaying isotopes (Visser et al., 2019).

5.3 Implications of TTD uncertainties

This study characterized the uncertainty in TTDs, which summarize the catchment's hydrologic transport behavior, and thereby comprise decisive information for water managers. The uncertainty in the predicted TT_{50} has relevant implications for both water quantity and quality; the larger the 95% CI in the simulated TT_{50} , the greater the difference in the TT_{50} values, which, ultimately, implies distinct water release and solute export dynamics (McDonnell et al., 2010).

Uncertainty in TTDs may be crucial for characterizing the catchment's response to climatic changes (Wilusz et al., 2017). Considering the increasing severity of droughts in the past decades (Dai, 2013), a catchment that largely releases young water might be more affected by droughts than a catchment whose stream is fed by relatively old water sources. A short TT_{50} reveals a low drought resilience of the catchment, which could limit streamflow generation processes and change the instream water quality status. Likewise, TTD uncertainty may affect the quantification of the modern groundwater age, i.e., groundwater younger than 50 years (Bethke and Johnson, 2008). According to (Jasecko, 2019), the correct identification of modern groundwater abundance and distribution can help determine its renewal (Le Gal La Salle et al., 2001; Huang et al., 2017), groundwater wells and depths most likely to contain contaminants (Visser et al., 2013; Opazo et al., 2016), and the part of the aquifer flushed more rapidly.

Uncertainty in TTDs also impacts on assessing the fate of dissolved solutes, such as nitrates (Yang, X. et al., 2018; Nguyen et al., 2021, 2022), pesticides (Holvoet et al., 2007; Lutz et al., 2017), and chlorides (Kirchner et al., 2000; Benettin et al., 2013). These solutes constitute a crucial source of diffuse water pollution in agricultural areas (Jiang et al., 2014; Kumar et al., 2020), as they are spread on the soil in large quantities especially during the growing season. Exposure time of solutes with the soil matrix has strong consequences for biogeochemical reactions, such as denitrification in the case of nitrates (Kolbe et al., 2019; Kumar et al., 2020). A short TT_{50} suggests that water can be rapidly conveyed to the stream network (Kirchner et al., 2001), with limited time for denitrification. This explains the elevated instream concentration and short-term impact of nitrate export compared to that of a longer TT_{50} , which is typically associated with old water release and low nitrate concentration (Nguyen et al., 2021). Similarly, pesticide transport is highly affected by the TTD uncertainty as a long TT_{50} suggests little pesticide degradation due to decreased microbial activity along deeper flowpaths (Rodríguez-Cruz et al., 2006). In other cases, a shorter TT_{50} may limit the time for degradation causing a peak in the instream concentration (Leu et al., 2004). Overall, a longer TT_{50} can delay or buffer the catchment's reactive solute response at the outlet (Dupas et al., 2016; Van Meter et al., 2017). This creates a long-term effect of hydrological legacies and a continuous problem with diffuse pollution of nitrates (Ehrhardt et al., 2019; Winter et al., 2020) and pesticides (Lutz et al., 2013), which can persist in the catchment for several years. Finally, TTD uncertainties also play an important role in chloride transport, although chlorides are commonly known to

365 be conservative (Svensson et al., 2012). A short TT_{50} may indicate rapid chloride mobilization, whereas a long TT_{50} implies
chloride persistence in groundwater; thereby chloride accumulates and is released at lower rates, with impacts on the ecosystem
functions, vegetation uptake and metabolism (Xu et al., 1999).

Understanding the uncertainty in TTDs is crucial for the aforementioned implications. While previous studies have used only
a specific SAS function and/or specific data fitting technique, here we show that there could be a wide range of different results
370 in terms of water ages, model performances and parameter uncertainty. This is due to the specific choice regarding SAS param-
eterization and tracer data interpolation. With this, we want to convey that uncertainty is omnipresent in TTD-based models,
and we need to recognise it, especially when dealing with sparse tracer data and multiple choices for model parameterization.
Therefore, we want to encourage future studies to explore these uncertainties in other catchments and different geophysical
settings, with the final aim to investigate whether these uncertainties may affect the conclusions of water quantity and quality
375 studies for management purposes.

6 Conclusions

This study explored the uncertainty in TTDs of streamflow, resulting from twelve model setups obtained from different SAS
parameterizations (i.e., PLTI, PLTV and BETATI), and reconstruction of the precipitation isotopic signature in time and space
via interpolation (step function vs. sine-fit, raw vs. kriged values).

380 We found satisfactory KGE values, whose differences across the tested setups were statistically significant, meaning that the
choice of the setup matters. As a consequence, distinct setups led to considerably different simulated TT_{50} values. The choice
between using time-variant or time-invariant SAS functions was crucial as the time-invariant functions generated a moderately
stable 95% CI of the estimated TT_{50} because of the constant water selection preference over time. These functions may be
more appropriate for those catchments experiencing relatively little seasonality in the hydrological conditions.

385 On the other hand, the time-variant SAS function captured the dynamics of the catchment wetness, resulting in a pronounced
seasonality of TT_{50} . However, the time-variant SAS function also produced a larger 95% CI in TT_{50} , notably during drier
periods, which might indicate the need to constrain the function with additional data (e.g., finer tracer data resolution, and/or
information on evapotranspiration and storage). Significant differences in TT_{50} were observed depending on the employed
temporal interpolations. Results from the sine interpolation must be interpreted carefully as they poorly reproduced flashy
390 events in precipitation, thus indicating that some more dynamic transport processes were not fully accounted for. Conversely,
the step function interpolation was able to better reproduce the measured $\delta^{18}O_p$ data. Dry conditions were another reason for
uncertainty as indicated by the high variance in the simulated TT_{50} values. Finally, the use of spatial interpolation methods
did not substantially affect the uncertainty in TT_{50} as there were no appreciable differences in the trend of the modeled results
between kriged and raw isotopes, although the 95% CI in TT_{50} was wider when using raw $\delta^{18}O_p$.

395 Our study provides new insights into TTD uncertainty when high-frequency tracer data are missing and the SAS framework
is used. Regardless of the degree of efficiency or uncertainty, the decision on which setup is more plausible depends on a full
conceptual knowledge of the catchment functioning. We consider the presented approach as potentially applicable to other

studies for enabling a better characterization of TTDs uncertainty, improving TTD simulations and, ultimately, informing water management. These aspects are particularly crucial in view of evermore extreme climatic conditions and increasing water pollution under global change.

Code and data availability. The model used in this study is presented at <https://doi.org/10.5194/gmd-11-1627-2018>. The iteratively re-weighted least squares (IRLS) method used to get modelled daily kriged and raw isotope ($\delta^{18}\text{O}$) in precipitation with the sine interpolation is presented at <https://doi.org/10.5194/hess-22-3841-2018>. Hydroclimatic time series, $\delta^{18}\text{O}$ data and interpolated $\delta^{18}\text{O}$ time series can be accessed at <https://doi.org/10.5281/zenodo.6630477>.

Author contributions. AB conducted the model simulations, the analysis and interpretation of the results, and wrote the original draft of the paper. SRL and RK designed and conceptualized the study, and provided data for model simulations. TVN provided technical support for modelling and helped organize the structure and content of the paper. AB, SRL, RK and TVN conceived the methodology and experimental design. All co-authors helped AB interpret the results. All authors contributed to the review, final writing and finalization of this work.

Competing interests. RK is a member of the editorial board of Hydrology and Earth System Sciences.

410 References

- Abbaspour, K. C., Johnson, C. A., and van Genuchten, M. T.: Estimating uncertain flow and transport parameters using a sequential uncertainty fitting procedure, *Vadose Zone Journal*, 3(4), 1340–1352, <https://doi.org/10.2136/vzj2004.1340>, 2004.
- Ajami, N. K., Duan, Q., and Sorooshian, S.: An integrated hydrologic Bayesian multimodel combination framework: Confronting input, parameter, and model structural uncertainty in hydrologic prediction, *Water Resour. Res.*, 43, W01403, <https://doi.org/10.1029/2005WR004745>, 2007.
- 415 Ambrose, B.: Variable 'active' versus 'contributing' areas or periods: a necessary distinction, *Hydrol. Process.*, 18, 1149–1155, <https://doi.org/10.1002/hyp.5536>, 2004.
- Andersson, J. C. M., Arheimer, B., Traoré, F., Gustafsson, D., , and Ali, A.: Process refinements improve a hydrological model concept applied to the Niger River basin, *Hydrol. Process.*, 31, 4540–4554, <https://doi.org/10.1002/hyp.11376>, 2017.
- 420 Asadollahi, M., Stumpp, C., Rinaldo, A., and Benettin, P.: Transport and water age dynamics in soils: A comparative study of spatially integrated and spatially explicit models, *Water Resour. Res.*, 56, e2019WR025539, <https://doi.org/10.1029/2019WR025539>, 2020.
- Benettin, P. and Bertuzzo, E.: tran-SAS v1.0: a numerical model to compute catchment-scale hydrologic transport using StorAge Selection functions, *Geosci. Model Dev.*, 11, 1627–1639, <https://doi.org/10.5194/gmd-11-1627-2018>, 2018.
- Benettin, P., van der Velde, Y., van der Zee, S. E. A. T. M., Rinaldo, A., and Botter, G.: Chloride circulation in a lowland catchment and the
425 formulation of transport by travel time distributions, *Water Resour. Res.*, 49, 4619–4632, <https://doi.org/10.1002/wrcr.20309>, 2013.
- Benettin, P., Bailey, S. W., Campbell, J. L., Green, M. B., Rinaldo, A., Likens, G. E., J., M. K., and Botter, G.: Linking water age and solute dynamics in streamflow at the Hubbard Brook Experimental Forest, NH, USA, *Water Resour. Res.*, 51, 9256–9272, <https://doi.org/10.1002/2015WR017552>, 2015a.
- Benettin, P., Kirchner, J. W., Rinaldo, A., and Botter, G.: Modeling chloride transport using travel time distributions at Plynlimon, Wales,
430 *Water Resour. Res.*, 51, 3259–3276, <https://doi.org/10.1002/2014WR016600>, 2015b.
- Benettin, P., Soulsby, C., Birkel, C., Tetzlaff, D., Botter, G., and Rinaldo, A.: Using SAS functions and high-resolution isotope data to unravel travel time distributions in headwater catchments, *Water Resour. Res.*, 53, 1864–1878, <https://doi.org/10.1002/2016WR020117>, 2017.
- Bethke, C. M. and Johnson, T. M.: Groundwater age and groundwater age dating, *Annu. Rev. Earth Planet. Sci.*, 36, 121–152, <https://doi.org/10.1146/annurev.earth.36.031207.124210>, 2008.
- 435 Beven, K.: A manifesto for the equifinality thesis, *J. Hydrol.*, 320, 18–36, <https://doi.org/10.1016/j.jhydrol.2005.07.007>, 2006.
- Beven, K. and Freer, J.: Equifinality, data assimilation, and uncertainty estimation in mechanistic modelling of complex environmental systems using the GLUE methodology, *J. Hydrol.*, 249, 11–29, [https://doi.org/10.1016/S0022-1694\(01\)00421-8](https://doi.org/10.1016/S0022-1694(01)00421-8), 2001.
- Birkel, C. and Soulsby, C.: Advancing tracer-aided rainfall-runoff modelling: A review of progress, problems and unrealised potential, *Hydrol. Process.*, 29, 5227–5240, <https://doi.org/10.1002/hyp.10594>, 2015.
- 440 Birkel, C., Dunn, S. M., Tetzlaff, D., and Soulsby, C.: Assessing the value of high-resolution isotope tracer data in the stepwise development of a lumped conceptual rainfall-runoff model, *Hydrol. Process.*, 24, 2335–2348, <https://doi.org/10.1002/hyp.7763>, 2010.
- Blume, T. and van Meerveld, H. J.: From hillslope to stream: methods to investigate subsurface connectivity, *WIREs Water*, 2, 177–198, <https://doi.org/10.1002/wat2.1071>, 2015.
- Botter, G., Bertuzzo, E., Bellin, A., and Rinaldo, A.: On the Lagrangian formulations of reactive solute transport in the hydrologic response,
445 *Water Resour. Res.*, 41, W04008, <https://doi.org/10.1029/2004WR003544>, 2005.

- Botter, G., Bertuzzo, E., and Rinaldo, A.: Transport in the hydrologic response: Travel time distributions, soil moisture dynamics, and the old water paradox, *Water Resour. Res.*, 46, W03 514, <https://doi.org/10.1029/2009WR008371>, 2010.
- Botter, G., Bertuzzo, E., and Rinaldo, A.: Catchment residence and travel time distributions: The master equation, *Geophys. Res. Lett.*, 38, L11 403, <https://doi.org/10.1029/2011GL047666>, 2011.
- 450 Buzacott, A. J. V., van der Velde, Y., Keitel, C., and Vervoort, R. W.: Constraining water age dynamics in a south-eastern Australian catchment using an age-ranked storage and stable isotope approach, *Hydrol. Process.*, 34, 4384–4403, <https://doi.org/10.1002/hyp.13880>, 2020.
- Dai, A.: Erratum: Increasing drought under global warming in observations and models, *Nature Clim Change*, 3, 171, <https://doi.org/10.1038/nclimate1811>, 2013.
- Danesh-Yazdi, M., Fofoula-Georgiou, E., Karwan, D. L., and Botter, G.: Inferring changes in water cycle dynamics of intensively managed landscapes via the theory of time-variant travel time distributions, *Water Resour. Res.*, 52, 7593–7614, <https://doi.org/10.1002/2016WR019091>, 2016.
- 455 Danesh-Yazdi, M., Klaus, J., Condon, L. E., and Maxwell, R. M.: Bridging the gap between numerical solutions of travel time distributions and analytical storage selection functions, *Hydrol. Process.*, 32, 1063–1076, <https://doi.org/10.1002/hyp.11481>, 2018.
- Yang, J., Heidbüchel, I., Musolff, A., Reinstorf, F., and Fleckenstein, J. H.: Exploring the Dynamics of Transit Times and Subsurface Mixing in a Small Agricultural Catchment, *Water Resour. Res.*, 54, 2317–2335, <https://doi.org/10.1002/2017WR021896>, 2018.
- 460 Yang, X., Seifeddine, J., Zink, M., Fleckenstein, J. H., Borchardt, D., and Rode, M.: A New Fully Distributed Model of Nitrate Transport and Removal at Catchment Scale, *Water Resour. Res.*, 54, 5856–5877, <https://doi.org/10.1029/2017WR022380>, 2018.
- Drever, M. C. and Hrachowitz, M.: Migration as flow: using hydrological concepts to estimate the residence time of migrating birds from the daily counts, *Methods Ecol. Evol.*, 8, 1146–1157, <https://doi.org/10.1111/2041-210X.12727>, 2017.
- 465 Dunn, S. M., Bacon, J. R., Soulsby, C., Tetzlaff, D., Stutter, M. I., Waldron, S., and Malcolm, I. A.: Interpretation of homogeneity in $\delta^{18}\text{O}$ signatures of stream water in a nested sub-catchment system in north-east Scotland, *Hydrol. Process.*, 22, 4767–4782, <https://doi.org/10.1002/hyp.7088>, 2008.
- Dupas, R., Jomaa, S., Musolff, A., Borchardt, D., and Rode, M.: Disentangling the influence of hydroclimatic patterns and agricultural management on river nitrate dynamics from sub-hourly to decadal time scales, *Sci. Total Environ.*, 571, 791–800, <https://doi.org/10.1016/j.scitotenv.2016.07.053>, 2016.
- 470 Dupas, R., Musolff, A., Jawitz, J. W., Rao, P. S. C., Jäger, C. G., Fleckenstein, J. H., Rode, M., and Borchardt, D.: Carbon and nutrient export regimes from headwater catchments to downstream reaches, *Biogeosciences*, 14, 4391–4407, <https://doi.org/10.5194/bg-14-4391-2017>, 2017.
- Ehrhardt, S., Kumar, R., Fleckenstein, J. H., Attinger, S., and Musolff, A.: Trajectories of nitrate input and output in three nested catchments along a land use gradient, *Hydrol. Earth Syst. Sci.*, 23, 3503–3524, <https://doi.org/10.5194/hess-23-3503-2019>, 2019.
- 475 Feng, X., Faiia, A. M., and Posmentier, E. S.: Seasonality of isotopes in precipitation: A global perspective, *J. Geophys. Res.*, 114, D08 116, <https://doi.org/10.1029/2008jd011279>, 2009.
- Gupta, H. V., Kling, H., Yilmaz, K. K., and Martinez, G. F.: Decomposition of the mean squared error and NSE performance criteria: Implications for improving hydrological modelling, *J. Hydrol.*, 377, 80–91, <https://doi.org/10.1016/j.jhydrol.2009.08.003>, 2009.
- 480 Harman, C. J.: Time-variable transit time distributions and transport: Theory and application to storage-dependent transport of chloride in a watershed, *Water Resour. Res.*, 51, 1–30, <https://doi.org/10.1002/2014WR015707>, 2015.
- Harman, C. J.: Age-Ranked Storage-Discharge Relations: A Unified Description of Spatially Lumped Flow and Water Age in Hydrologic Systems, *Water Resour. Res.*, 55, 7143–7165, <https://doi.org/10.1029/2017WR022304>, 2019.

- Heidbüchel, I., Yang, J., Musolff, A., Troch, P., Ferré, T., and Fleckenstein, J. H.: On the shape of forward transit time distributions in
485 low-order catchments, *Hydrol. Earth Syst. Sci.*, 24, 2895–2920, <https://doi.org/10.5194/hess-24-2895-2020>, 2020.
- Heidbüchel, I., Troch, P. A., and Lyon, S. W.: Separating physical and meteorological controls of variable transit times in zero-order catch-
ments, *Water Resour. Res.*, 49, 7644—7657, <https://doi.org/10.1002/2012WR013149>, 2013.
- Holvoet, K. M., Seuntjens, P., and Vanrolleghem, P. A.: Monitoring and modeling pesticide fate in surface waters at the catchment scale,
Ecol. Model., 209, 53–64, <https://doi.org/10.1016/j.ecolmodel.2007.07.030>, 2007.
- 490 Hrachowitz, M., Soulsby, C., Tetzlaff, D., Malcolm, I. A., and Schoups, G.: Gamma distribution models for transit time estimation in catch-
ments: Physical interpretation of parameters and implications for time-variant transit time assessment, *Water Resour. Res.*, 46, W10536,
<https://doi.org/10.1029/2010WR009148>, 2010.
- Hrachowitz, M., Soulsby, C., Tetzlaff, D., and Malcolm, I. A.: Sensitivity of mean transit time estimates to model conditioning and data
availability, *Hydrol. Process.*, 25, 980–990, <https://doi.org/10.1002/hyp.7922>, 2011.
- 495 Hrachowitz, M., Savenije, H., Bogaard, T. A., Tetzlaff, D., and Soulsby, C.: What can flux tracking teach us about water age distribution
patterns and their temporal dynamics?, *Hydrol. Earth Syst. Sci.*, 17, 533–564, <https://doi.org/10.5194/hess-17-533-2013>, 2013.
- Hrachowitz, M., Benettin, P., van Breukelen, B. M., Fovet, O., Howden, N. J. K., Ruiz, L van der Velde, Y., and Wade, A. J.: Transit times —
the link between hydrology and water quality at the catchment scale, *WIREs Water*, 3, 629–657, <https://doi.org/10.1002/wat2.1155>, 2016.
- Huang, T., Pang, Z., Li, J., Xiang, Y., and Zhao, Z.: Mapping groundwater renewability using age data in the Baiyang alluvial fan, NW,
500 China, *Hydrogeol J.*, 25, 743–755, <https://doi.org/10.1007/s10040-017-1534-z>, 2017.
- Jasechko, S., Wassenaar, L. I., and Mayer, B.: Isotopic evidence for widespread cold-season-biased groundwater recharge and young stream-
flow across central Canada, *Hydrol. Process.*, 31, 2196–2209, <https://doi.org/10.1002/hyp.11175>, 2017.
- Jasecko, S.: Global isotope hydrogeology — review, *Reviews of Geophysics*, 57, 835–965, <https://doi.org/10.1029/2018RG000627>, 2019.
- Jiang, S., Jomaa, S., and Rode, M.: Modelling inorganic nitrogen leaching in nested mesoscale catchments in central Germany, *Ecohydrol.*,
505 7, 1345–1362, <https://doi.org/10.1002/eco.1462>, 2014.
- Jing, M., Heße, F., Kumar, R., Kolditz, O., Kalbacher, T., and Attinger, S.: Influence of input and parameter uncertainty on the prediction of
catchment-scale groundwater travel time distributions, *Hydrol. Earth Syst. Sci.*, 23, 171–190, <https://doi.org/10.5194/hess-23-171-2019>,
2019.
- Kim, M. and Troch, P. A.: Transit time distributions estimation exploiting flow-weighted time: Theory and proof-of-concept, *Water Resour.*
510 *Res.*, 56, e2020WR027186, <https://doi.org/10.1029/2020WR027186>, 2022.
- Kim, M., Pangle, L. A., Cardoso, C., Lora, M., Volkmann, T. H. M., Wang, Y., Harman, C. J., and Troch, P. A.: Transit time distributions and
StorAge Selection functions in a sloping soil lysimeter with time-varying flow paths: Direct observation of internal and external transport
variability, *Water Resour. Res.*, 52, 7105–7129, <https://doi.org/10.1002/2016WR018620>, 2016.
- Kirchner, J. W.: Getting the right answers for the right reasons: Linking measurements, analyses, and models to advance the science of
515 hydrology, *Water Resour. Res.*, 42, W03S04, <https://doi.org/10.1029/2005WR004362>, 2006.
- Kirchner, J. W.: Aggregation in environmental systems – Part I: Seasonal tracer cycles quantify young water fractions, but not mean transit
times, in spatially heterogeneous catchments, *Hydrol. Earth Syst. Sci.*, 20, 279–297, <https://doi.org/10.5194/hess-20-279-2016>, 2016.
- Kirchner, J. W.: Quantifying new water fractions and transit time distributions using ensemble hydrograph separation: theory and benchmark
tests, *Hydrol. Earth Syst. Sci.*, 23, 303–349, <https://doi.org/10.5194/hess-23-303-2019>, 2019.
- 520 Kirchner, J. W., Feng, X., and Neal, C.: Fractal stream chemistry and its implications for contaminant transport in catchments, *Nature*, 403,
524–527, <https://doi.org/10.1038/35000537>, 2000.

- Kirchner, J. W., Feng, X., and Neal, C.: Catchment-scale advection and dispersion as a mechanism for fractal scaling in stream tracer concentrations, *J. Hydrol.*, 254, 82–101, [https://doi.org/10.1016/S0022-1694\(01\)00487-5](https://doi.org/10.1016/S0022-1694(01)00487-5), 2001.
- Kirchner, J. W., Feng, X., Neal, C., and Robson, A. J.: The fine structure of water-quality dynamics: the (high-frequency) wave of the future, *Hydrol. Process.*, 18, 1353–1359, <https://doi.org/10.1002/hyp.5537>, 2004.
- 525 Kolbe, T., de Dreuzy, J. R., Abbott, B. W., Aquilina, L., Babey, T., Green, C. T., et al.: Stratification of reactivity determines nitrate removal in groundwater, *Proceedings of the National Academy of Sciences*, 116(7), 2494–2499, <https://doi.org/10.1073/pnas.1816892116>, 2019.
- Kumar, R., Samaniego, L., and S., A.: The effects of spatial discretization and model parameterization on the prediction of extreme runoff characteristics, *J. Hydrol.*, 392, 54–69, <https://doi.org/10.1016/j.jhydrol.2010.07.047>, 2010.
- 530 Kumar, R., Samaniego, L., and Attinger, S.: Implications of distributed hydrologic model parameterization on water fluxes at multiple scales and locations, *Water Resour. Res.*, 49, 360–379, <https://doi.org/10.1029/2012WR012195>, 2013.
- Kumar, R., Heße, F., Rao, P. S. C., Musolff, A., Jawitz, J. W., Sarrazin, F., Samaniego, L., Fleckenstein, J. H., Rakovec, O., Thober, S., and Attinger, S.: Strong hydroclimatic controls on vulnerability to subsurface nitrate contamination across Europe, *Nature Communications*, 11, 6302, <https://doi.org/10.1038/s41467-020-19955-8>, 2020.
- 535 Le Gal La Salle, C., Marlin, C., Leduc, C., Taupin, J. D., Massault, M., and Favreau, G.: Renewal rate estimation of groundwater based on radioactive tracers (³H, ¹⁴C) in an unconfined aquifer in a semi-arid area, Iullemeden Basin, Niger, *J. Hydrol.*, 254, 145–156, [https://doi.org/10.1016/S0022-1694\(01\)00491-7](https://doi.org/10.1016/S0022-1694(01)00491-7), 2001.
- Leu, C., Singer, H., Stamm, C., Muller, S. R., and Schwarzenbach, R. P.: Simultaneous Assessment of Sources, Processes, and Factors Influencing Herbicide Losses to Surface Waters in a Small Agricultural Catchment, *Environ. Sci. Technol.*, 38, 3827–3834, <https://doi.org/10.1021/es0499602>, 2004.
- 540 Lutz, S., van Meerveld, H. J., Waterloo, M. J., Broers, H. P., and van Breukelen B. M.: A model-based assessment of the potential use of compound-specific stable isotope analysis in river monitoring of diffuse pesticide pollution, *Hydrol. Earth Syst. Sci.*, 17, 4505–4524, <https://doi.org/10.5194/hess-17-4505-2013>, 2013.
- Lutz, S. R., van der Velde, Y., Elsayed, O. F., Imfeld, G., Lefrancq, M., Payraudeau, S., and van Breukelen, B. M.: Pesticide fate on catchment scale: conceptual modelling of stream CSIA data, *Hydrol. Earth Syst. Sci.*, 21, 5243–5261, <https://doi.org/10.5194/hess-21-5243-2017>, 2017.
- 545 Lutz, S. R., Krieg, R., Müller, C., Zink, M., Knöller, K., Samaniego, L., and Merz, R.: Spatial patterns of water age: using young water fractions to improve the characterization of transit times in contrasting catchments, *Water Resour. Res.*, 54, 4767–4784, <https://doi.org/10.1029/2017WR022216>, 2018.
- 550 McDonnell, J. J., McGuire, K., Aggarwal, P., Beven, K. J., Biondi, D., Destouni, G., et al.: How old is streamwater? Open questions in catchment transit time conceptualization, modelling and analysis, *Hydrol. Process.*, 24, 1745–1754, <https://doi.org/10.1002/hyp.7796>, 2010.
- McGuire, K. J. and McDonnell, J. J.: A review and evaluation of catchment transit time modeling, *J. Hydrol.*, 330, 543–563, <https://doi.org/10.1016/j.jhydrol.2006.04.020>, 2006.
- 555 McKay, M. D., Beckman, R. J., and Conover, W. J.: A Comparison of Three Methods for Selecting Values of Input Variables in the Analysis of Output from a Computer Code, *Technometrics*, 21, 239–245, <https://doi.org/10.2307/1268522>, 1979.
- Morgenstern, U., Daughney, C. J., Leonard, G., Gordon, D., Donath, F. M., and Reeves, R.: Using groundwater age and hydrochemistry to understand sources and dynamics of nutrient contamination through the catchment into Lake Rotorua, New Zealand, *Hydrol. Earth Syst. Sci.*, 19, 803–822, <https://doi.org/10.5194/hess-19-803-2015>, 2015.

- 560 Nguyen, T. V., Kumar, R., Lutz, S. R., Musolff, A., Yang, J., and Fleckenstein, J. H.: Modeling Nitrate Export From a Mesoscale Catchment Using StorAge Selection Functions, *Water Resour. Res.*, 57, e2020WR028490, <https://doi.org/10.1029/2020WR028490>, 2021.
- Nguyen, T. V., Sarrazin, F. J., Ebeling, P., Musolff, A., Fleckenstein, J. H., and Kumar, R.: Toward Understanding of Long-Term Nitrogen Transport and Retention Dynamics Across German Catchments, *Geophysical Research Letters*, 49, e2022GL100278, 2022.
- Niemi, A. J.: Residence time distributions of variable flow processes, *The International Journal of Applied Radiation and Isotopes*, 28(10), 565 855–860, [https://doi.org/10.1016/0020-708X\(77\)90026-6](https://doi.org/10.1016/0020-708X(77)90026-6), 1977.
- Opazo, T., Aravena, R., and Parker, B.: Nitrate distribution and potential attenuation mechanisms of a municipal water supply bedrock aquifer, *Applied Geochemistry*, 73, 157–168, <https://doi.org/10.1016/j.apgeochem.2016.08.010>, 2016.
- Queloz, P., Carraro, L., Benettin, P., Botter, G., Rinaldo, A., and Bertuzzo, E.: Transport of fluorobenzoate tracers in a vegetated hydrologic control volume: 2. Theoretical inferences and modeling., *Water Resour. Res.*, 51, 2793–2806, <https://doi.org/10.1002/2014WR016508>, 570 2015.
- Rinaldo, A. and Marani, M.: Basin Scale Model of Solute Transport, *Water Resour. Res.*, 23, 2107–2118, <https://doi.org/10.1029/WR023i011p02107>, 1987.
- Rinaldo, A., Botter, G., Bertuzzo, E., Uccelli, A., Settin, T., and Marani, M.: Transport at basin scales: 1. Theoretical framework, *Hydrol. Earth Syst. Sci.*, 10, 19–29, <https://doi.org/10.5194/hess-10-19-2006>, 2006.
- 575 Rinaldo, A., Benettin, P., Harman, C. J., Hrachowitz, M., McGuire, K. J., van der Velde, Y., et al.: Storage selection functions: A coherent framework for quantifying how catchments store and release water and solutes, *Water Resour. Res.*, 51, 4840–4847, <https://doi.org/10.1002/2015WR017273>, 2015.
- Rodriguez, N. B., McGuire, K. J., and Klaus, J.: Time-Varying Storage–Water Age Relationships in a Catchment With a Mediterranean Climate, *Water Resour. Res.*, 54, 3988–4008, <https://doi.org/10.1029/2017WR021964>, 2018.
- 580 Rodriguez, N. B., Pfister, L., Zehe, E., and Klaus, J.: A comparison of catchment travel times and storage deduced from deuterium and tritium tracers using StorAge Selection functions, *Hydrol. Earth Syst. Sci.*, 25, 401–428, <https://doi.org/10.5194/hess-25-401-2021>, 2021.
- Rodríguez-Cruz, M. S., Jones, J. E., and Bending, G. D.: Field-scale study of the variability in pesticide biodegradation with soil depth and its relationship with soil characteristics, *Soil Biology and Biochemistry*, 38, 2910–2918, <https://doi.org/10.1016/j.soilbio.2006.04.051>, 2006.
- Samaniego, L., Kumar, R., and Attinger, S.: Multiscale parameter regionalization of a grid-based hydrologic model at the mesoscale, *Water Resour. Res.*, 46, W05523, <https://doi.org/10.1029/2008WR007327>, 2010.
- 585 Schoups, G., van de Giesen, N. C., and Savenije, H. H. G.: Model complexity control for hydrologic prediction, *Water Resour. Res.*, 44, W00B03, <https://doi.org/10.1029/2008WR006836>, 2008.
- Seeger, S. and Weiler, M.: Reevaluation of transit time distributions, mean transit times and their relation to catchment topography, *Hydrol. Earth Syst. Sci.*, 18, 4751–4771, <https://doi.org/10.5194/hess-18-4751-2014>, 2014.
- 590 Soulsby, C. and Tetzlaff, D.: Towards simple approaches for mean residence time estimation in ungauged basins using tracers and soil distributions, *J. Hydrol.*, 363, 60–74, <https://doi.org/10.1016/j.jhydrol.2008.10.001>, 2008.
- Stewart, M. K., Morgenstern, U., and McDonnell, J. J.: Truncation of stream residence time: How the use of stable isotopes has skewed our concept of streamwater age and origin, *Hydrol. Process.*, 24, 1646–1659, <https://doi.org/10.1002/hyp.7576>, 2010.
- Stewart, M. K., Morgenstern, U., McDonnell, J. J., and Pfister, L.: The ‘hidden streamflow’ challenge in catchment hydrology: A call to 595 action for stream water transit time analysis, *Hydrol. Process.*, 26, 2061–2066, <https://doi.org/10.1002/hyp.9262>, 2012.
- Stockinger, M. P., Lücke, A., McDonnell, J. J., Diekkrüger, B., Vereecken, H., and Bogaen, H. R.: Interception effects on stable isotope driven streamwater transit time estimates, *Geophys. Res. Lett.*, 42, 5299–5308, <https://doi.org/doi:10.1002/2015GL064622>, 2015.

- Sutanudjaja, E. H., Van Beek, R., Wanders, N., Wada, Y., Bosmans, J. H. C., et al.: PCR-GLOBWB 2: a 5 arcmin global hydrological and water resources model, *Geosci. Model Dev.*, 11, 2429–2453, <https://doi.org/10.5194/gmd-11-2429-2018>, 2018.
- 600 Svensson, T., Lovett, G. M., and Likens, G. E.: Is chloride a conservative ion in forest ecosystems?, *Biogeochemistry*, 107, 125–134, <https://doi.org/10.1007/s10533-010-9538-y>, 2012.
- Tetzlaff, D., Piovano, T. A., P., Smith, A., K., C. S., Marsh, P., Wookey, P. A., Street, L. E., and Soulsby, C.: Using stable isotopes to estimate travel times in a data-sparse Arctic catchment: Challenges and possible solutions, *Hydrol. Process.*, 32, 1936–1952, <https://doi.org/10.1002/hyp.13146>, 2018.
- 605 Thiemig, V., Rojas, R., Zombrano-Bigiarini, M., and De Roo, A.: Hydrological evaluation of satellite-based rainfall estimates over the Volta and Baro-Akobo Basin, *J. Hydrol.*, 499, 324–338, <https://doi.org/10.1016/j.jhydrol.2013.07.012>, 2013.
- Van der Velde, Y., De Rooij, G. H., Rozemeijer, J. C., Van Geer, F. C., and Broers, H. P.: Nitrate response of a lowland catchment: On the relation between stream concentration and travel time distribution dynamics, *Water Resour. Res.*, 46, W11534, <https://doi.org/10.1029/2010WR009105>, 2010.
- 610 van der Velde, Y., Torfs, P. J. J. F., van der Zee, S. E. A. T. M., and Uijlenhoet, R.: Quantifying catchment-scale mixing and its effect on time-varying travel time distributions, *Water Resour. Res.*, 48, W06536, <https://doi.org/10.1029/2011WR011310>, 2012.
- Van Meter, K. J., Basu, N. B., and Van Cappellen, P.: Two centuries of nitrogen dynamics: legacy sources and sinks in the Mississippi and Susquehanna river basins, *Global Biogeochemical Cycles*, 31, 2–23, <https://doi.org/10.1002/2016GB005498>, 2017.
- 615 Visser, A., Broers, H. P., Purtschert, R., Sültenfuß, J., and de Jonge, M.: Groundwater age distributions at a public drinking water supply well field derived from multiple age tracers (^{85}Kr , $^3\text{H}/^3\text{He}$, and ^{39}Ar), *Water Resour. Res.*, 49, 7778–7796, <https://doi.org/10.1002/2013WR014012>, 2013.
- Visser, A., Thaw, M., Deinhard, A., Bibby, R., Safeeq, M., Conklin, M., Esser, B., and van der Velde, Y.: Cosmogenic isotopes unravel the hydrochronology and water storage dynamics of the Southern Sierra critical zone, *Water Resour. Res.*, 55, 1429–1450, <https://doi.org/10.1029/2018WR023665>, 2019.
- 620 von Freyberg, J., Studer, B., and Kirchner, J. W.: A lab in the field: high-frequency analysis of water quality and stable isotopes in stream water and precipitation, *Hydrol. Earth Syst. Sci.*, 21, 1721–1739, <https://doi.org/10.5194/hess-21-1721-2017>, 2017.
- von Freyberg, J., Allen, S. T., Seeger, S., Weiler, M., and Kirchner, J. W.: Sensitivity of young water fractions to hydro-climatic forcing and landscape properties across 22 Swiss catchments, *Hydrol. Earth Syst. Sci.*, 22, 3841–3861, <https://doi.org/10.5194/hess-22-3841-2018>, 2018.
- 625 von Freyberg, J., Rücker, A., Zappa, M., Schlumpf, A., Studer, B., and Kirchner, J. W.: Four years of daily stable water isotope data in stream water and precipitation from three Swiss catchments, *Sci Data*, 9, 46, <https://doi.org/10.1038/s41597-022-01148-1>, 2022.
- Wang, S., Hrachowitz, M., Schoups, G., and Stumpp, C.: Stable water isotopes and tritium tracers tell the same tale: No evidence for underestimation of catchment transit times inferred by stable isotopes in SAS function models, *Hydrol. Earth Syst. Sci. Discuss.* [preprint], in review, <https://doi.org/10.5194/hess-2022-400>, 2022.
- 630 Wilusz, D. C., Harman, C. J., and Ball, W. P.: Sensitivity of Catchment Transit Times to Rainfall Variability Under Present and Future Climates, *Water Resour. Res.*, 53, 10231–10256, <https://doi.org/10.1002/2017WR020894>, 2017.
- Winter, C., Lutz, S. R., Musolff, A., Kumar, R., Weber, M., and Fleckenstein, J. H.: Disentangling the Impact of Catchment Heterogeneity on Nitrate Export Dynamics From Event to Long-Term Time Scales, *Water Resour. Res.*, 57, e2020WR027992, <https://doi.org/10.1029/2020WR027992>, 2020.

- 635 Wollschläger, U., Attinger, S., Borchardt, D., Brauns, M., Cuntz, M., Dietrich, P., et al.: The Bode hydrological observatory: a platform for integrated, interdisciplinary hydro-ecological research within the TERENO Harz/Central German Lowland Observatory, *Environmental Earth Sciences*, 76, 29, <https://doi.org/10.1007/s12665-016-6327-5>, 2017.
- Xu, G., Magen, H., Tarchitzky, J., and Kafkafi, U.: Advances in Chloride Nutrition of Plants, *Adv. Agron.*, 68, 97–150, [https://doi.org/10.1016/S0065-2113\(08\)60844-5](https://doi.org/10.1016/S0065-2113(08)60844-5), 1999.
- 640 Zink, M., Kumar, R., Cuntz, M., and Samaniego, L.: A high-resolution dataset of water fluxes and states for Germany accounting for parametric uncertainty, *Hydrol. Earth Syst. Sci.*, 21, 1769–1790, <https://doi.org/10.5194/hess-21-1769-2017>, 2017.